

# <sup>1</sup>H nuclear magnetic resonance metabolomic analysis of mammary tumors from lean and obese Zucker rats exposed to 7,12-dimethylbenz[a]anthracene

TRACY L. WHITEHEAD<sup>1,2</sup>, ANDY W. HOLLEY<sup>3</sup>, SOHEILA KOROURIAN<sup>1,2</sup>,  
SAEID SHAAF<sup>3</sup>, THOMAS KIEBER-EMMONS<sup>1,2</sup> and REZA HAKKAK<sup>2,3,4,5</sup>

<sup>1</sup>Department of Pathology, <sup>2</sup>Arkansas Cancer Research Center, Departments of <sup>3</sup>Dietetics and Nutrition,

<sup>4</sup>Pediatrics, University of Arkansas for Medical Sciences, Little Rock, AR 72205;

<sup>5</sup>Arkansas Children's Hospital Research Institute, Little Rock, AR 72202, USA

Received June 5, 2007; Accepted July 11, 2007

**Abstract.** Obesity increases mammary tumor development in Zucker rats following a single administration of the pro-carcinogen 7,12-dimethylbenz(a)anthracene (DMBA). Fifty-day-old obese and lean female Zucker rats were orally gavaged with 65 mg/kg DMBA and sacrificed 139 days post DMBA treatment. At the end of the experiment, mammary tumors were detected in 68% of the obese rats compared to 32% of the lean group (P<0.001). <sup>1</sup>H nuclear magnetic resonance (<sup>1</sup>H-NMR) spectra obtained for hydrophilic and lipophilic extracts from excised tumors illustrated fundamental differences in metabolic profiles between the two groups. Differences were observed for key choline compounds, namely phosphocholine and glycerophosphocholine, both markers of malignancy and apoptosis. In addition, levels of lactate, creatine, *myo*-inositol,  $\alpha$ -glucose, alanine, leucine, glutamate, glutamine, tyrosine, phenylalanine, and NADH varied between the lean and obese groups. Principal component analysis indicated class separation between tumors from lean and obese rats based on their metabolic

profiles, illustrating the potential for using <sup>1</sup>H-NMR metabolomic methods for identifying altered metabolic pathways. Our results suggest that obesity enhances the risk for DMBA-induced mammary tumor development in rats. However, the mechanism for this increase in risk is currently unknown and will require further studies for elucidation.

## Introduction

Obesity has been classified as an epidemic in the US for over two decades. Recent data suggest that the prevalence of overweight and obesity currently exceeds 66% among US adults with the rate rapidly increasing, particularly among children and young adolescents (1). Obesity has been associated with major causes of morbidity and mortality such as diabetes, cardiovascular disease and several types of cancer, including breast cancer (2). In fact, excess body weight has been related to almost 20% of all the cancer deaths in women and 14% of those in men in the US yearly (3). It is estimated that during 2007 almost 178,480 women will be diagnosed with invasive breast cancer, and 40,460 will eventually die from this disease (4). Epidemiological studies have linked breast cancer and obesity in postmenopausal women, with an estimated 3% increase in risk for each 1 kg/m<sup>2</sup> increase in BMI (5).

In animal models, elevated body weight has been associated with an increase in both spontaneous and chemically induced mammary tumors in various strains of mice (6-10). Experimentally, the Zucker rat (*fa/fa*) is the best known, most widely used rat model of genetic obesity. Obesity in the Zucker rat is inherited as an autosomal-recessive trait caused by a mutation (*fa*) in the leptin receptor gene (11,12). Animals homozygous for the *fa* allele become noticeably obese by age 3 to 5 weeks, and by 14 weeks of age more than 40% of their body is composed of lipids (13). Obese Zucker rats develop hyperinsulinemia and insulin resistance before they develop obesity-associated, non-insulin-dependent diabetes mellitus in a manner similar to that of humans, making them an excellent model for investigating the relationship between obesity and mammary tumor development (14).

---

*Correspondence to:* Dr Reza Hakkak, Department of Dietetics and Nutrition, University of Arkansas for Medical Sciences, 4301 West Markham Street, Mail Slot 627, Little Rock, AR 72205, USA  
E-mail: HakkakReza@uams.edu

**Abbreviations:** NMR, nuclear magnetic resonance; TSP, trimethylsilyl-2,2,3,3-tetradeuteriopropionic acid; ppm, part-per-million; PCA, principal component analysis; NOESY, nuclear Overhauser enhancement spectroscopy; PLS-DA, partial least-squares discriminant analysis; PCD, programmed cell death; PUFAs, polyunsaturated fatty acids; PAHs, polycyclic aromatic hydrocarbons; DMBA, 7,12-dimethylbenz[a]anthracene; PC, phosphocholine; GPC, glycerophosphocholine; mEH, microsomal epoxide hydrolase; BMI, body mass index

**Key words:** breast cancer, metabolomics, metabonomics, nuclear magnetic resonance, obesity

Lean Zucker rats, in contrast, exhibit normal metabolic function and are considered ideal controls.

While many investigators have used the Zucker rat model to study the development, etiology, associated pathogenesis, possible treatment, and putative mechanisms of severe obesity, this model has never been used to study DMBA-induced mammary carcinogenesis. DMBA is a polycyclic aromatic hydrocarbon (PAH) and known procarcinogen that is activated following oxidation via CYP1A1 and CYP1B1 activity to its ultimate carcinogenic form DMBA-3,4-dihydrodiol-1,2-epoxide (Fig. 1) (15-17). Upon activation, DMBA has been shown to be a potent inducer of mammary carcinoma in rodent model systems and is widely accepted as a model for its similarity to human breast cancer (18). To better understand the mechanisms that are associated with obesity and breast cancer development, we used 7,12-dimethylbenz[a]anthracene (DMBA)-exposed lean and obese Zucker rats as a model to investigate alterations that occur within the metabolic pathways of tumor cells developing in these two physiologically distinct classes.

Recently, we established that DMBA induces mammary tumors in obese female Zucker rats at a faster rate than in their lean counterparts (19). Obese animals had more than double the risk for developing DMBA-induced mammary tumors as well. Results from this study suggested that the induction of mammary carcinoma in obese female Zucker rats via exposure to DMBA parallels epidemiological data and is an appropriate model in which to investigate the mechanism(s) that underlie the role of obesity in mammary tumor development.

In continuance of those findings, we conducted a  $^1\text{H}$  nuclear magnetic resonance ( $^1\text{H}$ -NMR) metabolomics investigation of mammary tumors from both obese and lean Zucker rats in an attempt to define possible altered metabolic pathways based upon endogenous metabolite levels so as to provide a mechanistic explanation for why such dramatic differences in tumor growth rate and number are observed. By defining possible points of alteration in metabolic pathways, the link between obesity and breast cancer should become clearer, possibly suggesting new methods for disease treatment and/or prevention.

## Materials and methods

**Materials.** Deuterium oxide (99.9%  $\text{D}_2\text{O}$ ), methanol- $d_4$  ( $\text{CD}_3\text{OD}$ ), chloroform- $d$  ( $\text{CDCl}_3$ ), sodium 3-trimethylsilyl-2,2,3,3- $d_4$ -propionate (TSP), and 7,12-dimethylbenz[a]anthracene (DMBA) were purchased from Aldrich Chemical Co. (St. Louis, MO). Phosphate-buffered saline tablets (without calcium and magnesium) were purchased from MP Biomedicals, Inc. (Solon, OH).

**Preparation of tissue samples for NMR spectroscopy.** Frozen mammary tumors obtained from lean and obese Zucker rat littermates (19) were thawed and homogenized in 3-ml microfuge tubes using a Qiagen TissueLyser (Retsch GmbH, Haan, Germany). Polar and nonpolar metabolites were then extracted from the tissue using 3 ml of a methanol, chloroform, and water solvent mixture (2:2:1). Samples were vortexed for 60 sec followed by centrifugation at 1,000  $\times$  g for 15 min to

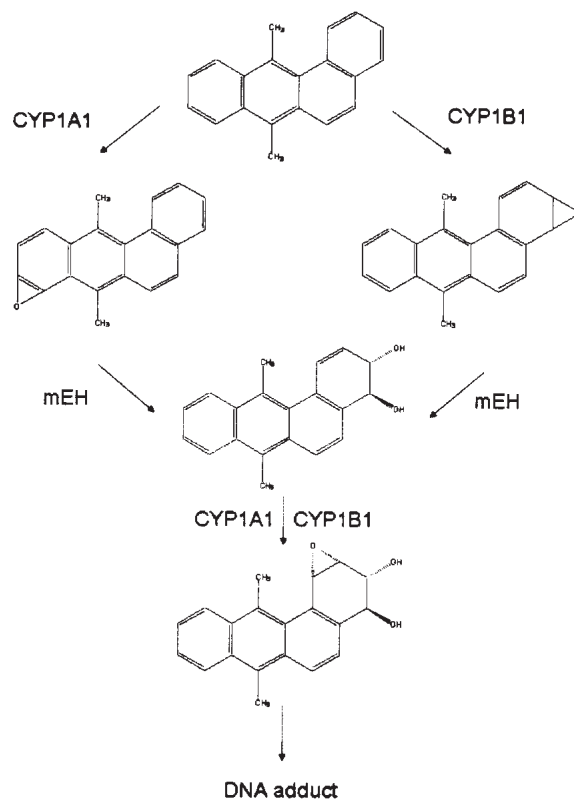


Figure 1. Biotransformation pathway for the procarcinogen 7,12-dimethylbenz[a]anthracene (DMBA, top) by cytochromes P450 CYP1B1, CYP1A1, and mEH (30).

separate layers. Aqueous and organic fractions were removed and transferred to clean glass vials by pipette, and the procedure was repeated. Vials were placed in a Savant SpeedVac (Thermo Electron Corp., Waltham, MA, USA) and evaporated to dryness overnight. Polar metabolites were redissolved in 1 ml of  $\text{D}_2\text{O}$  and were evaporated to dryness once again. All samples were stored in capped vials at  $-80^\circ\text{C}$ .

Immediately prior to NMR analysis, polar tissue extracts were re-suspended in 520  $\mu\text{l}$  of a 0.1 M sodium phosphate buffer (in 99.9%  $\text{D}_2\text{O}$ ; pH, 7.4) containing 0.5 mM sodium 3-trimethylsilyl-2,2,3,3- $d_4$ -propionate (TSP) as an internal chemical shift standard. For nonpolar tissue extracts, 520  $\mu\text{l}$  of a 2:1 mixture of  $\text{CDCl}_3$ : $\text{CD}_3\text{OD}$  containing 0.5 mM tetramethylsilane (TMS) as an internal chemical shift standard was used to re-suspend samples for analysis. All samples were centrifuged at 1000  $\times$  g for 5 min, and 500  $\mu\text{l}$  of each solution were transferred to 5-mm NMR tubes for analysis.

**$^1\text{H}$ -NMR spectroscopic analysis of samples.**  $^1\text{H}$ -NMR spectra of tissue extracts were acquired using a Varian Inova 800 MHz spectrometer equipped with a cold probe and operating at a proton frequency of 799.73 MHz at a temperature of  $25^\circ\text{C}$ . One-dimensional  $^1\text{H}$  data were collected without spinning, and solvent suppression of the residual water resonance was achieved using a 1D NOESY (NOESYpresat, 'tnnoesy') experiment. Spectra were collected with 128 transients using a  $90^\circ$  pulse and an 11.50  $\mu\text{sec}$  pulse width, a saturation delay of 3  $\mu\text{sec}$ , an acquisition time of 3.336 sec, a

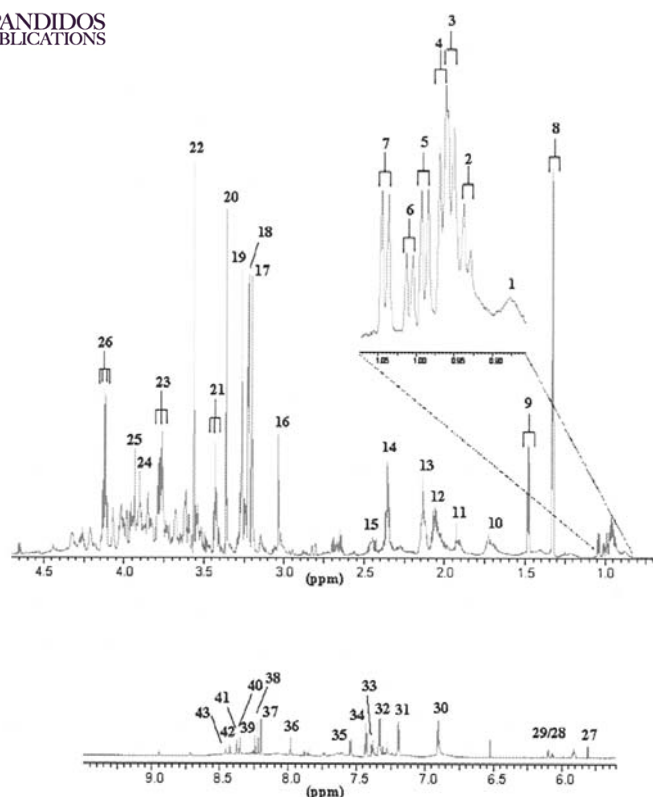


Figure 2.  $^1\text{H}$ -NMR spectra (800 MHz) of aqueous soluble metabolites extracted from mammary tumors excised from lean female Zucker rats exposed to DMBA. Assignments correspond to Table I.

sweep width of 12 ppm, and 32 K complex data points, resulting in a total acquisition time of ~15 min per spectrum.

**Pre-processing of NMR spectra.** All datasets were zero-filled to 64 K data points, and exponential line broadenings of 0.3 Hz were applied before Fourier transformation. All spectra were automatically phased, baseline corrected using a quadratic function, and calibrated (TSP at 0.00 ppm) using the 1D NMR processor module in ACD SpecManager (version 9.0; Advanced Chemistry Development, Toronto, ON, Canada). Next, the spectral region between 10 to 0.5 parts per million (ppm) was divided into 1122 integral slices, each 0.01 ppm in width using the ACDLabs Intelligent Binning feature within ACD SpecManager. To eliminate the effect of variations in water resonance suppression in polar samples, the spectral region spanning 5.0-4.7 ppm was set to an integral value of zero. Binned spectra intensity data were then formatted into a spreadsheet using Microsoft Excel for subsequent principal component analysis (PCA) and partial least-squares discriminant analysis (PLS-DA).

**Multivariate spectral analysis.** PCA of the pre-processed NMR data was conducted using the multivariate data analysis software SIMCA-P+ (version 11.0.0, Umetrics, Umeå, Sweden). All frequency regions were scaled to the total spectral integrated area, followed by mean-centering and pareto-scaling, a method which assigns each component in the dataset a variance that is numerically equal to its own standard deviation. Following PCA, additional chemometric

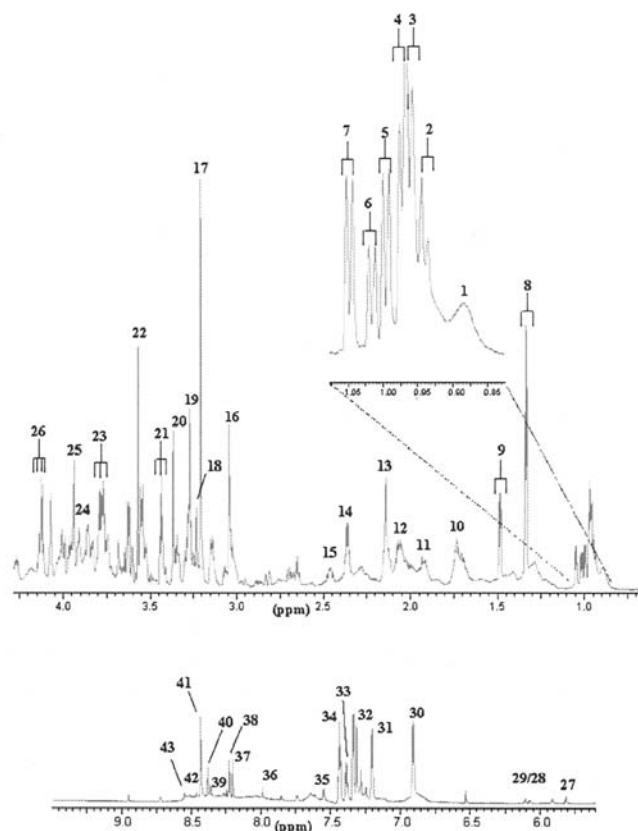


Figure 3.  $^1\text{H}$ -NMR spectra (800 MHz) of aqueous soluble metabolites extracted from mammary tumors excised from obese female Zucker rats exposed to DMBA. Assignments correspond to Table I.

analyses using PLS-DA were conducted to determine which metabolites were responsible for class separation.

## Results

### $^1\text{H}$ -NMR spectra of tumor extracts from lean and obese rats.

$^1\text{H}$ -NMR spectra obtained for metabolites present in aqueous tissue extract fractions indicated subtle differences between levels of certain key metabolites that are commonly associated with energy pathways. Aqueous extracts from tumors excised from lean Zucker rats (Fig. 2) indicated elevated levels of the metabolites lactate ( $\delta$  1.33), alanine ( $\delta$  1.49), isoleucine ( $\delta$  2.06) and glutamate ( $\delta$  2.36) when compared to similar extracts obtained from tumors excised from obese Zucker rats (Fig. 3). In contrast, tumor extracts from obese animals indicated elevated levels of the metabolites leucine ( $\delta$  0.96), glutamine ( $\delta$  2.14), creatine ( $\delta$  3.04), *myo*-inositol ( $\delta$  4.06), and choline-containing compounds (choline,  $\delta$  3.20; PC/GPC,  $\delta$  3.26) as shown in Fig. 3. Tentative chemical shift assignments for several metabolites identified in lean and obese aqueous tissue extracts based on a combination of literature assignments (22) and spectral data collected for pure metabolites are provided in Table I.

$^1\text{H}$ -NMR spectra obtained for metabolites present in organic tissue extract fractions also indicated notable differences between lean and obese subjects, with obese Zucker rat tumors containing lower levels of unsaturated fatty acids when compared to lean littermates, in particular,

Table I. Tentative  $^1\text{H}$  chemical shift assignment of Zucker rat mammary tumors. Chemical shift referencing is relative to TSP (0.00 ppm).

Number	Metabolite	Moiety	Chemical shift (lean)	Chemical shift (obese)
1	Fatty acids	$-\text{CH}_3$	0.88	0.88
2	Isoleucine	$\delta\text{CH}_3$	0.93	0.93
3	Leucine	$\delta'\text{CH}_3$	0.95	0.96
4	Leucine	$\delta\text{CH}_3$	0.96	0.97
5	Valine	$\gamma\text{CH}_3$	0.99	0.99
6	Isoleucine	$\gamma\text{CH}_3$	1.01	1.01
7	Valine	$\gamma'\text{CH}_3$	1.04	1.04
8	Lactate	$\text{CH}_3$	1.33	1.33
9	Alanine	$\text{CH}_3$	1.48	1.48
10	Fatty acids		1.71	1.71
11	Acetate	$(\text{CH}_3)$	1.92	1.92
12	Isoleucine	$\beta\text{CH}$	2.05	2.06
13	Glutamine	$\beta\text{CH}_2$	2.14	2.14
14	Glutamate	$\gamma\text{CH}_2$	2.36	2.36
15	Glutamine	$\gamma\text{CH}_2$	2.45	2.46
16	Creatine	$\text{CH}_3$	3.03	3.04
17	Choline	$\text{N}(\text{CH}_3)_3$	3.20	3.20
18	Phosphocholine	$\text{N}(\text{CH}_3)_3$	3.23	3.22
19	Taurine	$\text{N}-\text{CH}_2$	3.26	3.27
20	<i>scyllo</i> -Inositol		3.36	3.36
21	Taurine	$\text{S}-\text{CH}_2$	3.43	3.43
22	Glycine	$\alpha\text{CH}_2$	3.56	3.57
23	Alanine	$\alpha\text{CH}_2$	3.77	3.78
24	Aspartate	$\alpha\text{CH}_2$	3.90	3.90
25	Creatine	$\text{CH}_2$	3.93	3.93
26	Lactate	$\text{CH}$	4.12	4.12
27	Uracil	$\text{C}_6\text{H}$ , ring	5.81	5.81
28	NADH	$\text{N}1'\text{H}$	6.07	6.08
29	NADH	$\text{A}1'\text{H}$	6.11	6.11
30	Tyrosine	$\text{C}_3\text{H}, 5\text{H}$ ring	6.91	6.91
31	Tyrosine	$\text{C}_2\text{H}, 6\text{H}$ ring	7.20	7.20
32	Phenylalanine	$\text{C}_2\text{H}, \text{C}_6\text{H}$ ring	7.33	7.34
33	Phenylalanine	$\text{C}_4\text{H}$ , ring	7.38	7.38
34	Phenylalanine	$\text{C}_3\text{H}, \text{C}_5\text{H}$ ring	7.43	7.44
35	Unknown	Doublet	7.55	7.55
36	Histidine	$\text{C}_2\text{H}$ , ring	7.99	7.99
37	NADH	$\text{N}5$ ring	8.21	8.21
38	Inosine	$\text{C}_2$ ring	8.22	8.22
39	Inosine	$\text{C}_8$ ring	8.36	8.36
40	NADH	$\text{A}8\text{H}$ ring	8.43	8.43
41	Formate	$\text{HCOO}'$	8.46	8.46
42	ADP	$\text{C}_8$ ring	8.53	ND
43	ATP	$\text{C}_8$ ring	8.55	ND

decreased NMR resonances indicative of  $-\text{CH}=\text{CH}-$  ( $\delta$  5.35) and  $-\text{CH}=\text{CHCH}_2\text{CH}=\text{CH}-$  ( $\delta$  2.78) functional groups and elevated levels of methylene ( $\delta$  1.27), cholesterol ( $\delta$  0.70), and the phospholipid functional group  $-\text{N}^+(\text{CH}_3)_3$  commonly associated with choline-containing compounds (Fig. 4).

*Chemometric analysis of tumor extract data.* PCA analysis of the reduced spectra indicated good separation between lean and obese populations when comparing both aqueous and organic tumor extracts. The models correctly separated all lean subjects from all obese subjects as shown in Fig. 5. The



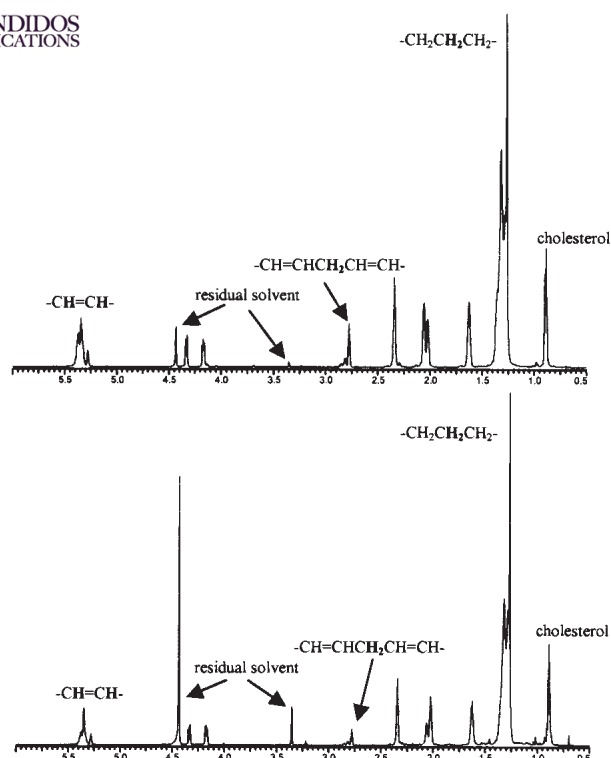


Figure 4. Comparison of  $^1\text{H}$ -NMR spectra of organic soluble metabolites extracted from mammary tumors described in Figs. 2 and 3. The top figure illustrates organic soluble metabolites extracted from an obese female Zucker rat tumor, while the bottom is from a lean female Zucker rat tumor.

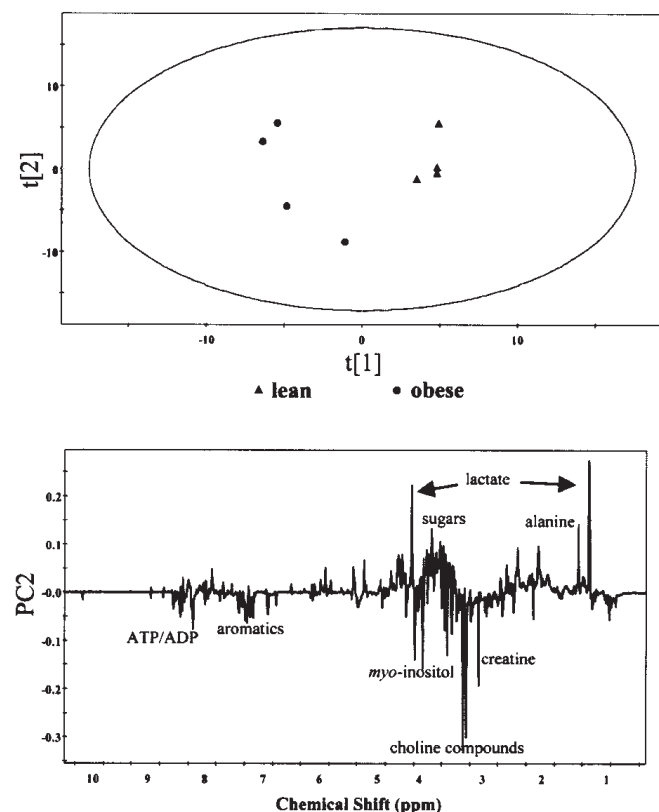


Figure 5. Partial least-squares discriminant analysis (PLS-DA) score plot (top) and corresponding loading plot (bottom) indicating class separation between aqueous soluble tumor metabolite extracts from lean and obese rats and metabolites responsible for class separation.

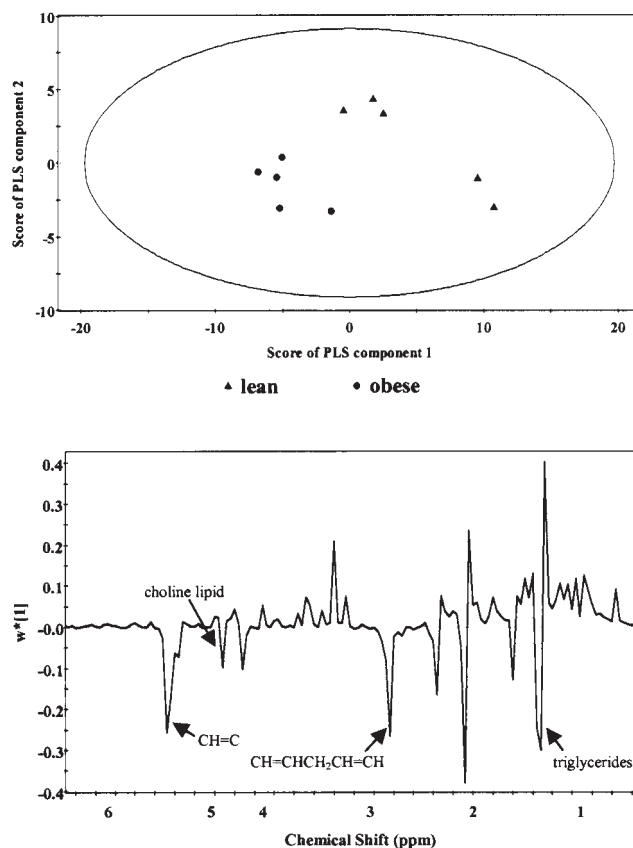


Figure 6. Partial least-squares discriminant analysis (PLS-DA) score plot (top) and corresponding loading plot (bottom) indicating class separation between organic soluble tumor metabolite extracts from lean and obese rats and metabolites responsible for class separation.

dataset obtained for lean Zucker rats displayed variables that were more tightly grouped, indicating less variability from one sample to the next. The dataset for obese Zucker rats displayed more variability, possibly due to additional systemic alterations in rats bearing more advanced levels of carcinoma or suffering from metabolic syndrome. Overall, attempts to discriminate between the two populations of Zucker rats by comparison of datasets indicated that PCA successfully distinguished between lean and obese tumor-bearing Zucker rats when using the first and second principal components.

*Loadings responsible for spectral differences between tumors.* In light of the fact that separation between tumor extracts from lean and obese tumor-bearing Zucker rats occurred when using unsupervised PCA, we attempted to identify which molecules were responsible for the differences in the observed spectral patterns. This was achieved by conducting PLS-DA and examining the resulting loading plot. The PLS-DA score plot and corresponding loading plot (Figs. 6 and 7) displayed NMR chemical shifts of molecules that were responsible for the separation of data sets along the two principal component factors shown. As can be seen, PLS components that were primarily responsible for class separation were those previously mentioned in the discussion of differences in NMR spectra; primarily lactate, choline, phosphocholine, and several amino acids from aqueous extracts (Fig. 6) and  $-\text{CH}=\text{CH}-$  and  $-\text{CH}=\text{CHCH}_2\text{CH}=\text{CH}-$  from organic extracts (Fig. 7).

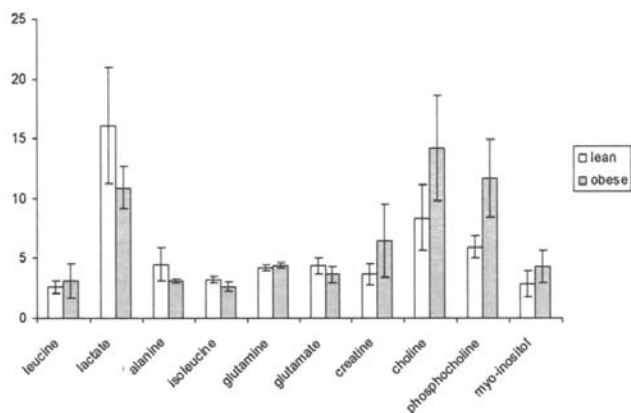


Figure 7. Most abundant metabolites identified in aqueous soluble tumor extracts. Bars indicate average metabolite concentration levels normalized against total NMR spectra intensity (95% CI).

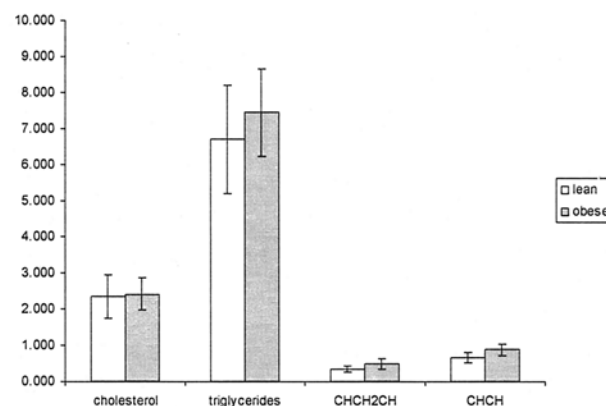


Figure 8. Most abundant metabolites identified in organic soluble tumor extracts. Bars indicate average metabolite concentration levels normalized against total NMR spectra intensity (95% CI).

## Discussion

To further investigate the role of obesity on tumor progression and the potential for using NMR metabolomics as a method for characterizing alterations in endogenous metabolic profiles in cancer-bearing organisms, we used  $^1\text{H}$ -NMR spectroscopy to analyze tumor extracts from an accepted model system for breast cancer, the DMBA-exposed rodent. Specifically, our main objective was to investigate and define the metabolic profiles of DMBA-induced mammary tumors in lean and obese Zucker rats with an ultimate goal of linking obesity to increased mammary tumor metabolism and tumorigenesis in the context of up- and down-regulated metabolites.

NMR-based metabolomics is a technique that is capable of globally analyzing biological samples with relative ease and little modification, eliminating the need to measure individual linewidths or identify metabolites which give rise to certain resonances. The application of NMR metabolomics to the analysis of serum for markers indicative of cancer is one potential new method being explored for early cancer detection. Recently, NMR metabolomic methods were successfully applied to patient serum and were shown to be capable of discriminating between women with epithelial ovarian cancer and healthy controls (20). In a similar fashion, we showed that this method can also distinguish between mouse models of mammary carcinoma and healthy controls (21).

To compensate for extremely complicated NMR spectra consisting of overlapping resonances from hundreds of possible metabolites, metabolomics involves the application of a combination of data reduction techniques and complex multivariate statistical analysis methods. Chemometric techniques such as principal component analysis (PCA) and partial least-squares discriminant analysis (PLS-DA) are some of the more well-established techniques that have been used in  $^1\text{H}$ -NMR metabolomic analysis of complex biological NMR spectra with success.

An early study of breast cancer applied such multivariate data analysis methods to NMR data in order to correlate the presence of various metabolites in human breast tissue with different stages of mammary tumor development. Both

tumors and non-involved breast tissue were obtained from 16 patients prior to undergoing surgery. Samples were analyzed for 10 metabolites to evaluate whether or not tumor types could be quickly determined based on concentrations of those metabolites. Results indicated that tumor tissue contains elevated levels of choline, and upon closer examination, that the major contributors to the choline peaks in the NMR spectra of extracts from invasive cancers result from both phosphocholine (PCho) and glycerophosphocholine (GPC). In addition, phosphoethanolamine (PE) and taurine also appeared to contribute significantly to those spectra as well, making them potentially useful as indicators of malignancy. Glucose was found to be less prevalent in malignant tissue as opposed to healthy tissue, presumably due to the high rate of aerobic glycolysis known to exist within tumors (22).

Metabolically, elevated total choline levels in tissue are indicative of cellular growth, inflammation, and migratory status, all signs of tumor cell proliferation and angiogenesis (23). In addition, alterations in cellular choline levels have been linked to cellular death processes as well, due to the fact that high proliferation rates in cancer cells are associated with a rapid rate of membrane turnover, leading to high concentrations of membrane precursors as well as catabolites containing choline (24). In general, malignant lesions have a tendency to display elevated levels of composite choline compounds when compared to benign lesions. The ratio of phosphocholine to glycerophosphocholine has been shown to be increased in cases of malignancy as well (25). End-products of glycolytic metabolism such as lactate are also key markers of tumor progression, while metabolic products of the TCA cycle are diminished or often non-existent.

In the present study, we applied the methods of  $^1\text{H}$ -NMR-based metabolomics to the analysis of metabolic profiles for aqueous and organic extracts obtained from tumors developing in both lean and obese Zucker rats following exposure to the procarcinogen DMBA. In doing so, we observed that there were fundamental differences in many of the key metabolites commonly associated with cancer. With respect to choline compounds, which are typically elevated in tumor cells when compared to normal cells, we observed that tumors excised from obese Zucker rats contained elevated levels of choline-containing metabolites when compared to

SPANDIDOS  
PUBLICATIONS

cised from lean littermates. In particular, phospho- levels were higher in obese Zucker rats when compared to lean. Elevated phosphocholine levels have been shown to be directly linked to indicators of more aggressive tumor phenotypes including metastatic ability (26); therefore, tumors taken from obese Zucker rats appear to have a more aggressive metabolic phenotype when compared to lean littermates, suggesting that obesity enhances tumor aggressiveness.

Differences in lactate levels between tumors obtained from obese rats versus lean rats could potentially be explained in the context of tumor cell energetics. For some time, there has been debate over whether tumor cells may gain some advantage using aerobic glycolysis as opposed to oxidation to derive energy (27). While complete oxidation of glucose to CO<sub>2</sub> in the process of mitochondrial respiration would result in a yield of ATP that is 18 times per molecule of glucose greater than that of aerobic glycolysis, one of the classic markers for tumor cell metabolite profiles that has been consistent throughout many studies, is an elevated level of lactate. This feature of tumor cell metabolism suggests that further breakdown of lactate to yield ATP production may not be necessary for many tumors to survive; simply excreting lactate back to the host and obtaining glucose of aerobic glycolysis might be sufficient for tumor maintenance.

Some have argued that aerobic glycolysis may be favored over oxidation due to a lack of mitochondria within the tumor (27). Based on the metabolites identified within this study, it appears that tumor cells excised from obese rats may have undergone some degree of oxidative respiration. This is illustrated by a large decrease in free lactate and higher levels of ATP+ADP when compared to tumors from lean rats. These data suggest that, in the early stages of tumorigenesis, aerobic glycolysis may be the dominant mechanism for energy production, while in the latter stages of tumor development oxidative respiration may become more important. This is suggested based on the fact that tumors develop in obese rats in half the time when compared to lean littermates (19). Based on their extended growth period due to an earlier start, a decrease in blood flow to the core of the larger tumor may result in a lack of incoming glucose, forcing the tumor to utilize respiration as a means for energy molecule production. However, without further functional mitochondrial and enzymatic studies this cannot be considered as fact and must at this point remain speculation.

As mentioned earlier, elevated levels of choline-containing compounds might also be explained in terms of the advanced age of these tumors and could be indicative of increased cell membrane turnover. A recent study applying <sup>1</sup>H-NMR analysis to lipid constituents of BT4C gliomas undergoing induced programmed cell death (PCD) demonstrated increases in polyunsaturated fatty acids (PUFAs), primarily the -CH=CH- resonance at 5.3 ppm and the -CH=CHCH<sub>2</sub>CH=CH- resonance at 2.8 ppm, corresponding to 18:1 and 18:2 lipids (28). It was suggested that increases in these lipids were the result of the breakdown products of cellular constituents, possibly mitochondrial membrane degradation, lipid droplet development, and autophagic vacuole development (29).

Linking these results to our own, it is possible that the observation of increased -CH=CH- and -CH=CHCH<sub>2</sub>CH=CH- resonances in the organic soluble tumor extracts from obese

rats may be indicative of the progression of PCD. Thus, our observations of metabolites possibly indicative of oxidative metabolism and lipids possibly indicative of PCD onset suggest that tumor cells may have the ability to change their metabolic processes relative to their age, suggesting that NMR spectroscopy may provide an additional mechanism for assessing tumor cell age and metabolic status.

In conclusion, we demonstrated that NMR spectroscopy coupled with chemometric analyses can distinguish between mammary tumor extracts obtained from lean and obese Zucker rats exposed to DMBA. Metabolic profiles for endogenous metabolites were unique to each class, suggesting that mammary tumor cells in obese rodents have altered mechanisms for energy derivation and cellular development when compared to those obtained from lean littermates. Several NMR-detectable metabolites suggest that tumors in obese rodents develop in a more rapid and aggressive manner, strengthening the argument that obesity and breast cancer are linked. NMR spectroscopy is an additional tool which may help to better define the mechanisms of this relationship in the future.

### Acknowledgements

The authors wish to acknowledge the Susan G. Komen Foundation and the Arkansas Bioscience Institute for funding for R.H. and the Department of Defense Breast Cancer Initiative (DAMD17-01-1-0366) and the National Institute of Health (CA089480) for funding for T.K-E. The authors wish to thank Phaedra Yount for the valuable assistance in the preparation of this manuscript.

### References

- Wyatt SB, Winters KP and Dubbert PM: Overweight and obesity: prevalence, consequences, and causes of a growing public health concern. *Am J Med Sci* 331: 166-174, 2006.
- Bray SG and Bellanger T: Epidemiology, trends, and morbidities of obesity and the metabolic syndrome. *Endocrine* 29: 109-117, 2006.
- Calle EE, Rodriguez C, Walker-Thurmond K and Thun MJ: Overweight, obesity, and mortality from cancer in a prospectively studied cohort of U.S. adults. *N Engl J Med* 348: 1625-1638, 2003.
- American Cancer Society: Cancer Facts and Figures 2007. American Cancer Society, Atlanta, 2007.
- Endogenous Hormones Breast Cancer Collaborative Group: Body mass index, serum sex hormones, and breast cancer risk in postmenopausal women. *J Natl Cancer Inst* 95: 1218-1226, 2003.
- Ballard-Barbash R and Swanson CA: Body weight: estimation of risk for breast and endometrial cancers. *Am J Clin Nutr* 63: 437S-441S, 1996.
- Waxler SH, Tabar P and Melcher LR: Obesity and the time of appearance of spontaneous mammary carcinoma in C3H mice. *Cancer Res* 13: 276-278, 1953.
- Waxler S: Obesity and cancer susceptibility in mice. *Am J Clin Nutr* 8: 760-766, 1960.
- Haseman JK, Bourbina J and Eustis SL: Effect of individual housing and other experimental design factors on tumor incidence in B6C3F1 mice. *Fundam Appl Toxicol* 23: 44-52, 1994.
- Wolff GL, Kodell RL, Cameron AM and Medina D: Accelerated appearance of chemically induced mammary carcinomas in obese yellow (A<sup>vy</sup>/A) (BALB/c X VY) F1 hybrid mice. *J Toxicol Environ Health* 10: 131-142, 1982.
- Tartaglia LA, Dembski M, Weng X, Deng N, Culpepper J, Devos R, Richards GJ, Campfield LA, Clark FT, Deeds J, *et al*: Identification and expression cloning of a leptin receptor, OB-R. *Cell* 83: 1263-1271, 1995.

12. Chua SC Jr, Chung WK, Wu-Peng XS, Zhang Y, Liu SM, Tartaglia L and Leibel RL: Phenotypes of mouse diabetes and rat fatty due to mutations in the OB (leptin) receptor. *Science* 271: 994-996, 1996.
13. Zucker LM: Fat mobilization *in vitro* and *in vivo* in the genetically obese Zucker rat 'fatty'. *J Lipid Res* 13: 234-243, 1972.
14. Bray GA: The Zucker-fatty rat: a review. *Fed Proc* 36: 148-153, 1977.
15. Christou M, Moore CJ, Gould MN and Jefcoate CR: Induction of mammary cytochromes P-450: an essential first step in the metabolism of 7,12-dimethylbenz(a)anthracene by rat mammary epithelial cells. *Carcinogenesis* 8: 73-80, 1987.
16. Dipple A: DNA adducts of chemical carcinogens. *Carcinogenesis* 16: 437-441, 1995.
17. Shimada T, Hayer C, Yamazaki H, Amin S, Hecht S, Guengerich F and Sutte T: Activity of chemically diverse pre-carcinogens by human cytochrome P-450 1B1. *Cancer Res* 56: 2979-2984, 1996.
18. Thompson HJ and Singh M: Rat models of premalignant breast disease. *J Mammary Gland Biol Neoplasia* 5: 409-420, 2000.
19. Hakkak R, Holley AW, MacLeod SL, Simpson PM, Fuchs GJ, Jo CH, Kieber-Emmons T and Korourian S: Obesity promotes 7,12-dimethylbenz(a)anthracene-induced mammary tumor development in female Zucker rats. *Breast Cancer Res* 7: R627-R633, 2005.
20. Odunsi K, Wollman RM, Ambrosone CB, Hutson A, McCann SE, Tammela J, Geisler JP, Miller G, Sellers T, Cliby W, Qian F, Keitz B, Intengan M, Lele S and Alderfer JL: Detection of epithelial ovarian cancer using <sup>1</sup>H-NMR-based metabolomics. *Int J Cancer* 113: 782-788, 2005.
21. Whitehead TL, Monzavi-Karbassi B and Kieber-Emmons T: <sup>1</sup>H-NMR metabolomics analysis of sera distinguishes between mammary tumor bearing mice and healthy controls. *Metabolomics* 1: 269-278, 2005.
22. Sitter B, Sonnewald U, Spraul M, Fjösne HE and Gribbestad IS: High-resolution magic angle spinning MRS of breast cancer tissue. *NMR Biomed* 15: 327-337, 2002.
23. Ackerstaff E, Glunde K and Bhujwala ZM: Choline phospholipid metabolism: A target in cancer cells? *J Cell Biochem* 90: 525-533, 2003.
24. Glunde K, Ackerstaff E, Natarajan K, Artemov D and Bhujwala ZM: Real-time changes in <sup>1</sup>H and <sup>31</sup>P NMR spectra of malignant human mammary epithelial cells during treatment with the anti-inflammatory agent indomethacin. *Magn Reson Med* 48: 819-825, 2002.
25. Aboagye EO and Bhujwala ZM: Malignant transformation alters membrane choline phospholipid metabolism of human mammary epithelial cells. *Cancer Res* 59: 80-84, 1999.
26. Seenu V, Pavan Kumar MN, Sharma U, Gupta SD, Mehta SN and Jagannathan NR: Potential of magnetic resonance spectroscopy to detect metastasis in axillary lymph nodes in breast cancer. *Magn Reson Imaging* 23: 1005-1010, 2005.
27. Stubbs M, Bashford CL and Griffiths JR: Understanding the tumor metabolic phenotype in the genomic era. *Curr Mol Med* 3: 49-59, 2003.
28. Griffin JL, Lehtimäki KK, Valonen PK, Gröhn OHJ, Kettunen MI, Ylä-Herttua S, Pitkänen A, Nicholson JK and Kauppinen RA: Assignment of <sup>1</sup>H nuclear magnetic resonance visible polyunsaturated fatty acids in BT4C gliomas undergoing ganciclovir-thymidine kinase gene therapy-induced programmed cell death. *Cancer Res* 63: 3195-3201, 2003.
29. Delikatny EJ, Cooper WA, Brammah S, Sathasivam N and Rideout DC: Nuclear magnetic resonance-visible lipids induced by cationic lipophilic chemotherapeutic agents are accompanied by increased lipid droplet formation and damaged mitochondria. *Cancer Res* 62: 1394-1400, 2002.
30. Gonzalez FJ and Kimura S: Understanding the role of xenobiotic-metabolism in chemical carcinogenesis using gene knockout mice. *Mutat Res* 477: 79-87, 2001.